

# Identification of the $D_{3h}$ Isomer of Carbon Trioxide ( $\text{CO}_3$ ) and Its Implications for Atmospheric Chemistry

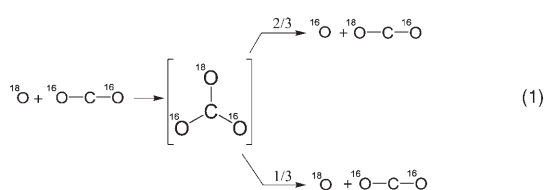
Corey S. Jamieson,<sup>[a]</sup> Alexander M. Mebel,<sup>[b]</sup> and Ralf I. Kaiser<sup>\*[a]</sup>

The  $\text{CO}_3$  molecule is considered an important reaction intermediate in the atmospheres of Earth and Mars for quenching electronically excited oxygen atoms and in contributing to the anomalous  $^{18}\text{O}$  isotope enrichment. The geometry of the  $\text{CO}_3$  intermediate plays an important role in explaining these effects; however, only the cyclic ( $C_{2v}$ ) isomer has been experimentally confirmed so

far. Here, we report on the first spectroscopic detection of the acyclic ( $D_{3h}$ ) isomer of carbon trioxide ( $^{12}\text{C}^{16}\text{O}_3$ ) via its  $\nu_1$  and  $\nu_2$  vibrational modes centered around  $1165\text{ cm}^{-1}$  under matrix isolation conditions; the identification of the  $^{12}\text{C}^{18}\text{O}_3$ ,  $^{13}\text{C}^{16}\text{O}_3$ ,  $^{13}\text{C}^{18}\text{O}_3$ ,  $^{16}\text{O}^{12}\text{C}^{18}\text{O}_2$ , and  $^{18}\text{O}^{12}\text{C}^{16}\text{O}_2$  isotopomers of the acyclic isomer confirms the assignments.

## 1. Introduction

For more than four decades, the structural isomers of the carbon trioxide molecule ( $\text{CO}_3$ ) have received considerable attention. Whether considering chemistry in the atmospheres of Venus, Earth, or Mars, or in the ices of the Martian polar caps and in comets, these isomers are essential in understanding the nonthermal chemistry of the carbon dioxide molecule ( $\text{CO}_2$ ) and the inherent  $^{18}\text{O}$  isotope enrichment of stratospheric carbon dioxide.<sup>[1–4]</sup> In view of radiation-induced degradation of oxygen-bearing molecules such as ozone or carbon dioxide, ionizing radiation from the solar wind can liberate oxygen atoms in their electronic ground ( $^3\text{P}$ ) or first electronically excited state ( $^1\text{D}$ ), both with a significant amount of excess kinetic energy. It was suggested that these atoms reacted with carbon dioxide molecules either in the gas phase<sup>[5–7]</sup> or in the solid state<sup>[8–10]</sup> to form a carbon trioxide intermediate(s) [Eq. (1)].



An isotopically labeled oxygen ( $^{18}\text{O}$ ) reactant has been introduced to keep track of the isotope exchange pathways. If the  $\text{CO}_3$  intermediate is not stabilized by a third-body collision, it may dissociate into oxygen and carbon dioxide, possibly quenching an electronically excited oxygen atom or undergoing isotope exchange of the oxygen atoms. These pathways have been included in atmospheric models to explain the  $^{18}\text{O}$  isotope enrichment of stratospheric carbon dioxide on Earth<sup>[11–14]</sup> and the regeneration of carbon dioxide on Mars, both in the upper atmosphere<sup>[15,16]</sup> and catalyzed in solid carbon dioxide ices.<sup>[17]</sup> However, despite the importance of the carbon trioxide isomers in atmospheric chemistry, to date only the  $C_{2v}$  symmetric structure has been observed experimentally

via low-temperature spectroscopy.<sup>[8–10]</sup> This molecule consists of a three-membered ring system (OCO) and a carbonyl functional group where the  $\pi$ -bond is localized to the C–O bond. The  $\text{CO}_3(D_{3h})$  molecule is characterized by three resonance structures (Figure 1), resulting in a delocalized  $\pi$ -bond over the three C–O bonds. The  $D_{3h}$  isomer lies only  $0.4\text{ kJ mol}^{-1}$  higher in energy than the  $C_{2v}$  structure with an isomerization barrier

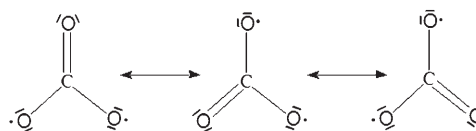


Figure 1. The three resonance forms for the  $D_{3h}$  isomer of carbon trioxide.

of  $18.4\text{ kJ mol}^{-1}$ .<sup>[18]</sup> Evidence for an interconversion of both structures first came when Baulch and Breckenridge, using isotopic labeling, found that an attacking oxygen atom has an approximately statistical (2/3) chance of being incorporated into the carbon dioxide molecule [Eq. (1)].<sup>[19]</sup> With the long lifetime of the  $\text{CO}_3$  intermediate, sufficient time could exist to access the  $D_{3h}$  structure and equally distribute the excess energy into the internal modes of freedom, giving each oxygen atom a nearly statistical probability of being ejected from the  $D_{3h}$  isomer.<sup>[18]</sup> However, the inclusion of the  $D_{3h}$  isomer into the  $^{18}\text{O}$  isotope exchange models is only theoretical, making investiga-

[a] C. S. Jamieson, Prof. R. I. Kaiser  
Department of Chemistry, University of Hawaii at Manoa  
Honolulu, HI 96822 (USA)  
Fax: (+808) 956-5908  
E-mail: kaiser@gold.chem.hawaii.edu

[b] Prof. A. M. Mebel  
Department of Chemistry and Biochemistry, Florida International University  
Miami FL 33199 (USA)

Supporting information for this article is available on the WWW under <http://www.chemphyschem.org> or from the author.

tion into the physical properties of the  $CO_3$  intermediate and the elementary mechanisms and kinetics of the reactions involved in  $^{18}O$  isotope enrichment difficult. Consequently, confirming the existence of the  $D_{3h}$  isomer would be a crucial step in validating this isomerization mechanism from the  $C_{2v}$  structure that is necessary in explaining the isotope exchange experiments. Also, if a one-step mechanism for the formation of the  $D_{3h}$  isomer was found via the reaction of an oxygen atom with a carbon dioxide molecule, it would provide an alternative, hitherto neglected, pathway for quenching  $O(^1D)$  atoms and  $^{18}O$  enrichment in the atmospheres of Earth, Mars, and Venus.

We present the first detection of the  $D_{3h}$  isomer of carbon trioxide formed via the reaction of energetic oxygen atoms with carbon dioxide molecules in low-temperature carbon dioxide samples utilizing infrared spectroscopy and combining these data with theoretical computations of the vibrational modes of these species. We also aim to understand the formation and isomerization pathways of both carbon trioxide isomers by analyzing the kinetics of the reactions, the mechanism(s) of formation, and the energetics associated with the potential-energy surface (PES). Finally, we comment on the implications of these findings for the atmospheric chemistries of Mars, Venus, and Earth.

## Experimental Section

The experiments were performed under matrix isolation conditions via radiolysis of carbon dioxide ices in a contamination-free ultra-high-vacuum stainless-steel chamber. The chamber can reach pressures down to  $5 \times 10^{-11}$  Torr by use of a magnetically suspended turbo molecular pump that is backed by a scroll pump. All pumps used are oil-free to ensure no hydrocarbon contaminants enter the system. Temperatures of 10 K are reached using a two-stage closed-cycle helium refrigerator that is interfaced directly to a polished single-crystal silver mirror onto which the ices are condensed. The silver substrate is suspended by a differentially pumped rotatable feedthrough, which aligns the wafer in the center of the main chamber. Gas condensation is carried out at 10 K where the pressure is regulated by a thermostatic valve that lets gas through the linear transfer mechanism and to the gas capillary array that discharges the gas evenly. The carbon dioxide gases were condensed for 3 min at a pressure of  $1.0 \times 10^{-7}$  Torr at 10 K to a total thickness of  $650 \pm 150$  nm. The ice sample was then irradiated isothermally with 5 keV electrons to cleave the carbon–oxygen double bond of carbon dioxide. The electron beam was actually operated at a nominal current of  $1 \mu A$  with an extraction efficiency of 78.8% and scanned over the sample area of  $1.8 \pm 0.3$  cm<sup>2</sup> to avoid heating the ice. The sample was irradiated for one hour, which exposed the target to  $1.8 \times 10^{16}$  electrons ( $1.0 \times 10^{16}$  electrons cm<sup>-2</sup>); longer irradiation times and higher beam currents should be avoided to eliminate overlapping electron trajectories and heating of the ice surface. Five experiments were performed using: a)  $CO_2$  (BOC, 99.999%), b)  $C^{18}O_2$  (CIL,  $^{18}O_2$  95%), c)  $^{13}CO_2$  (CIL,  $^{13}C$  99%), d)  $^{13}C^{18}O_2$  (CIL,  $^{13}C$  99%  $^{18}O_2$  90%), and e) a  $CO_2 : C^{18}O_2$  (1:1) ice mixture. The progress of the reaction was monitored using a Nicolet 510 DX Fourier transform infrared spectrometer (FTIR). The spectrometer has a wavenumber range of 6000–500 cm<sup>-1</sup> and operates in absorption–reflection–absorption mode with a reflection angle of 75° from the normal, relative to

the mirror surface. The infrared spectra of the ice were recorded online and in situ at an integrated time of 2.5 min and a resolution of 2 cm<sup>-1</sup>. One blank was also performed using the same experimental conditions as the  $CO_2$  experiment (a) but without irradiating the sample. The nondetection of bands that were assigned to the  $CO_3$  isomers confirms that they are the result of the radiolysis of  $CO_2$ .

Ab initio calculations of vibrational wavenumbers and infrared intensities were carried out using the multi-reference complete-active-space self-consistent field (CASSCF) method with the active space containing 16 electrons distributed at 13 orbitals and with the 6-311G(d) basis set. The calculations were performed by employing the DALTON program package<sup>[20]</sup> and are an extension of previous work carried out by Mebel et al.<sup>[18]</sup>

## 2. Results and Discussion

### 2.1. Infrared Band Assignments

First, we prove the assignment of the  $CO_3(D_{3h})$  molecule by investigating the absorption features that are observed in the infrared spectrum after the irradiation of the carbon dioxide ices. To confirm the assignments of the  $CO_3$  isotopomers, ab initio calculations are performed at the CASSCF(16,13)/6-311G(d) level of theory<sup>[20]</sup> (Supporting Information, Table S1). In the  $^{12}C^{16}O_2$  irradiation experiment, the  $CO_3(D_{3h})$  molecule is identified by a peak centered at 1165 cm<sup>-1</sup> (Figure 2), corresponding to the degenerate  $\nu_1/\nu_2$  vibrational modes. This band position

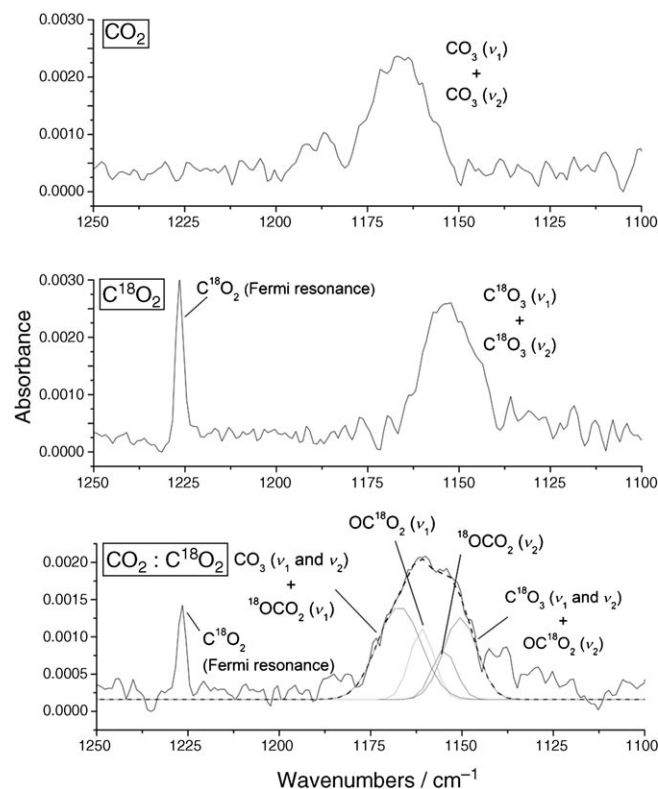


**Figure 2.** Representative infrared spectra (1250–1100 cm<sup>-1</sup>) for the  $\nu_1$  and  $\nu_2$  vibrational modes of the acyclic  $CO_3$  molecule after one hour of irradiation for the  $CO_2$ ,  $C^{18}O_2$ , and  $CO_2:C^{18}O_2$  experiments. The overlapping vibrational modes of four acyclic  $CO_3$  isotopomers are deconvoluted in the  $CO_2:C^{18}O_2$  experiment.

matches the calculated position of  $1168\text{ cm}^{-1}$  after being scaled by a factor of 0.97 (Table 1). This correction is necessary to account for the anharmonicity of the vibrations, which are

tion of one or two oxygen atoms in  $^{12}\text{C}^{16}\text{O}_3$  by  $^{18}\text{O}$  reduces the symmetry from  $D_{3h}$  to  $C_{2v}$ . This eliminates the degeneracy of the  $\nu_1$  and  $\nu_2$  modes (Table 1). Note that the  $\nu_1$  and  $\nu_2$  vibra-

tional modes have the largest infrared intensities; the  $\nu_4$  band holds the third largest infrared absorption coefficient and is calculated to be about half as intense as the degenerate  $\nu_1$  and  $\nu_2$  bands combined; due to this low intensity, the  $\nu_4$  band is not observed in our experiments. Summarized, eight isotopomers of the acyclic  $\text{CO}_3$  isomer have been identified in low-temperature carbon dioxide samples by comparing the experimentally observed peak positions with the computed data after scaling the predicted peak positions by 0.98–0.97.

To validate the quality of the calculations, a comparison with the known vibrational modes of the cyclic  $C_{2v}$  structure of carbon trioxide are made. In four of the carbon dioxide irradiation experiments ( $^{12}\text{C}^{16}\text{O}_2$ ,  $^{12}\text{C}^{18}\text{O}_2$ ,  $^{13}\text{C}^{16}\text{O}_2$ , and  $^{13}\text{C}^{18}\text{O}_2$ ), the cyclic carbon trioxide molecule is observed by four vibrational modes: its  $\nu_1$ ,  $\nu_2$ , and  $\nu_5$  fundamentals, and a Fermi resonance band between the  $\nu_1$  and  $2\nu_5$  modes (except for the  $\nu_2$  band of  $^{13}\text{C}^{18}\text{O}_3$ , which was not detected); for a more in-depth discussion of these assignments see Bennett et al.<sup>[10]</sup> The experimentally derived positions are compared with the theoretically calculated ab initio values (Table 1).

computed within the harmonic approximation. In the  $^{12}\text{C}^{18}\text{O}_2$  system, the  $\nu_1/\nu_2$  bands are red-shifted to  $1152\text{ cm}^{-1}$ . This agrees well with the computed value of  $1155\text{ cm}^{-1}$  after scaling by 0.98. Considering the  $^{13}\text{C}^{16}\text{O}_2$  irradiation experiment, the overlapping  $\nu_1$  and  $\nu_2$  bands of the  $^{13}\text{C}^{16}\text{O}_3$  molecule are found at  $1141\text{ cm}^{-1}$ , which agrees nicely with the calculated wavenumber of  $1139\text{ cm}^{-1}$  (0.97 scaling factor). Also, in the  $^{13}\text{C}^{18}\text{O}_2$  irradiation experiment, the  $^{13}\text{C}^{18}\text{O}_3$  molecule is identified by a band at  $1121\text{ cm}^{-1}$  compared to the computed and scaled position of  $1126\text{ cm}^{-1}$  (0.98 scaling factor). Note that in the  $^{12}\text{C}^{16}\text{O}_2/^{12}\text{C}^{18}\text{O}_2$  ice mixture, four acyclic isotopomers are formed:  $^{12}\text{C}^{16}\text{O}_3$ ,  $^{18}\text{O}^{12}\text{C}^{16}\text{O}_2$ ,  $^{16}\text{O}^{12}\text{C}^{18}\text{O}_2$ , and  $^{12}\text{C}^{18}\text{O}_3$  (Table 1; Figure 2). The overlapping  $\nu_1$  and  $\nu_2$  vibrational modes result in a broad peak centered at  $1158\text{ cm}^{-1}$  that is deconvoluted into the fundamental modes for the four isotopomers. The substitu-

For the  $\nu_1$  vibrations of the eight identified isotopomers the scaling factors are found to be between 0.97 and 0.99. The  $\nu_2$  and  $\nu_5$  modes have scaling factors of 0.99–1.00 and 0.94–0.95, respectively. These ranges demonstrate the expected consistency of our calculations. In the case of the acyclic  $\text{CO}_3$  molecule, a comparison of the experimental versus theoretical wavenumbers gave scaling factors varying from 0.97 to 0.98, which agrees with the precision found for the cyclic  $\text{CO}_3$  calculations. The actual scaling factor is dependent on the degree of anharmonicity present in the given vibration due to the differing anharmonicities in the vibrations. With the high reliability demonstrated from our calculations of the cyclic  $\text{CO}_3$  isomer and the matching precision of the acyclic  $\text{CO}_3$  calculations, this confirms our assignments of the  $\nu_1$  and  $\nu_2$  vibrational modes of the acyclic  $\text{CO}_3$  structure.

**Table 1.** The observed positions of the  $\nu_1$  and  $\nu_2$  vibrational modes of the acyclic  $\text{CO}_3$  isotopomers and the  $\nu_1$ ,  $\nu_2$  and  $\nu_5$  modes of cyclic  $\text{CO}_3$  are compared with the scaled theoretical wavenumbers calculated at the CASSCF(16,13)/6-311G(d) level of theory. The scaling factors between the observed and theoretical values are also reported. For the cyclic  $C_{2v}$  isotopomers, the last two oxygen atoms in parentheses form the COO cycle.

Isotopomer	Vibrational mode	Scaled wavenumber [cm <sup>-1</sup> ]	Observed wavenumber [cm <sup>-1</sup> ]	Scaling factor
acyclic $\text{CO}_3$				
$^{12}\text{C}^{16}\text{O}_3$	$\nu_1/\nu_2$	1168	1165	0.97
$^{12}\text{C}^{18}\text{O}_3$	$\nu_1/\nu_2$	1155	1152	0.98
$^{13}\text{C}^{16}\text{O}_3$	$\nu_1/\nu_2$	1139	1141	0.97
$^{13}\text{C}^{18}\text{O}_3$	$\nu_1/\nu_2$	1126	1121	0.98
$^{18}\text{O}^{12}\text{C}^{16}\text{O}_2$	$\nu_1$	1168	1167	0.97
$^{18}\text{O}^{12}\text{C}^{16}\text{O}_2$	$\nu_2$	1154	1155	0.97
$^{16}\text{O}^{12}\text{C}^{18}\text{O}_2$	$\nu_1$	1162	1161	0.97
$^{16}\text{O}^{12}\text{C}^{18}\text{O}_2$	$\nu_2$	1144	1150	0.97
cyclic $\text{CO}_3$				
$^{12}\text{C}^{16}\text{O}_3$	$\nu_1$	2041	2043	0.98
	$\nu_2$	1067	1067	1.00
	$\nu_5$	977	972	0.95
$^{16}\text{O}^{12}\text{C}^{18}\text{O}^{16}\text{O}$	$\nu_1$	2039	2039	0.98
	$\nu_2$	1058	–	–
	$\nu_5$	1016	–	–
$^{16}\text{O}^{12}\text{C}^{18}\text{O}_2$	$\nu_1$	2038	2029	0.97
	$\nu_2$	1035	–	–
	$\nu_5$	1012	–	–
$^{18}\text{O}^{12}\text{C}^{16}\text{O}_2$	$\nu_1$	2029	2021	0.99
	$\nu_2$	1049	–	–
	$\nu_5$	1028	–	–
$^{18}\text{O}^{12}\text{C}^{18}\text{O}^{16}\text{O}$	$\nu_1$	2007	2015	0.98
	$\nu_2$	1039	–	–
	$\nu_5$	1011	–	–
$^{12}\text{C}^{18}\text{O}_3$	$\nu_1$	2005	2006	0.98
	$\nu_2$	1014	1014	1.00
	$\nu_5$	960	955	0.95
$^{13}\text{C}^{16}\text{O}_3$	$\nu_1$	1986	1989	0.98
	$\nu_2$	1067	1067	1.00
	$\nu_5$	941	944	0.94
$^{13}\text{C}^{18}\text{O}_3$	$\nu_1$	1949	1953	0.98
	$\nu_2$	1011	–	–
	$\nu_5$	933	932	0.95

## 2.2. Kinetics and Dynamics

Having identified the acyclic isomer of carbon trioxide based on the  $\nu_1$  and  $\nu_2$  fundamentals of the six isotopomers and the wavenumber shifts supported by the theoretical calculations, we attempt now to investigate the formation pathways of this molecule. To do this, column densities from the  $^{12}C^{16}O_2$  experiment were calculated<sup>[10]</sup> for the observed molecular species after the one-hour irradiation. The temporal development of the column densities of the  $C_{2v}$  and  $D_{3h}$  isomers of carbon trioxide are shown in Figure 3. The reaction model shown in Figure 4 kinetically relates the observed molecular species and solves the rate constants for the synthesis and destruction of the  $CO_3(D_{3h})$  molecule.<sup>[21]</sup> The desired rate constants are obtained using the solution mapping technique<sup>[22]</sup> where the reaction model responses are fitted to a series of simple algebraic equations that are based on the rate equations and assigned active variables (Supporting Information, Table S2).

The radiation-induced dissociation of carbon dioxide initiates the reaction sequence by producing a carbon monoxide molecule and an oxygen atom that can be electronically excited ( $^1D$  state) and/or suprathreshold in its electronic ground state ( $^3P$ ), as shown in Equation (2).

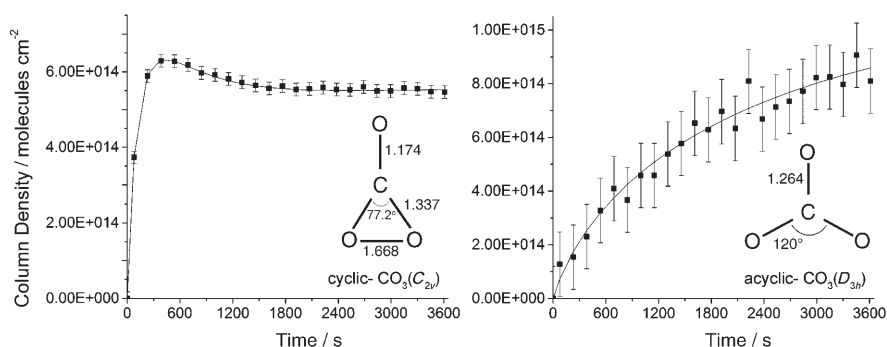
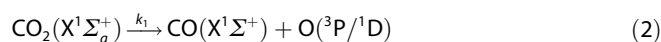


**Figure 3.** Column densities (molecules  $cm^{-2}$ ) of the two  $CO_3$  isomers ( $C_{2v}$  and  $D_{3h}$ ) plotted over one hour of irradiation for  $^{12}C^{16}O_2$ . The data are fitted according to the proposed reaction model. Error bars are derived by integrating a featureless region of the infrared spectrum and carrying that deviation through the column density calculations for each molecule (errors:  $D_{3h}$  isomer  $\pm 1.2 \times 10^{14}$  molecules  $cm^{-2}$ ,  $C_{2v}$  isomer  $\pm 1.7 \times 10^{13}$  molecules  $cm^{-2}$ ). Structures for the two isomers of carbon trioxide along with the calculated bond lengths (Å) and bond angles are also shown.

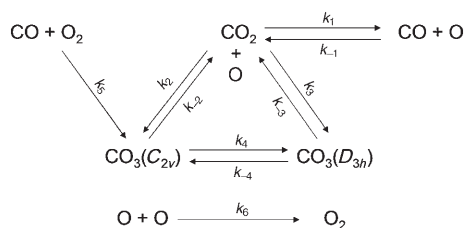
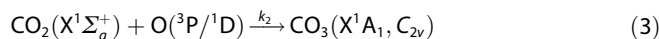
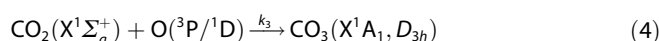


**Figure 4.** Kinetic reaction model, relating the observed molecules in the one-hour irradiation of carbon dioxide ice. Only species directly relevant to the production of the carbon trioxide isomers are included.

The rate for dissociation of carbon dioxide ( $k_1$ ) is  $4.1 \times 10^{-4} s^{-1}$  while the reverse reaction reforming carbon dioxide occurs at the rate  $k_{-1} = 1.4 \times 10^{-14} cm^2 molecule^{-1} s^{-1}$ . The oxygen atoms can react with adjacent carbon dioxide molecules in the ice, thereby forming carbon trioxide. The pathway to the  $C_{2v}$  isomer is experimentally known<sup>[5,6,8-10]</sup> [Equation (3)].



The reaction is exoergic by  $197.3 kJ mol^{-1}$  relative to  $CO_2 + O(^1D)$ . The rate of formation of the  $C_{2v}$  isomer of carbon trioxide ( $k_2$ ) is  $6.4 \times 10^{-17} cm^2 molecule^{-1} s^{-1}$ ; the destruction rate of  $CO_3(C_{2v})$  is fitted to  $8.3 \times 10^{-3} s^{-1}$  ( $k_{-2}$ ). Based on our experimental detection of the  $D_{3h}$  isomer, a direct pathway of formation via the  $CO_2 + O$  reaction ( $k_3$ ) has to be added to the reaction model, see Equation (4).



This reaction is exoergic by  $196.9 kJ mol^{-1}$  relative to  $CO_2 + O(^1D)$ . The rate constant for the production of  $CO_3(D_{3h})$ ,  $k_3$ , was calculated to be  $9.4 \times 10^{-18} cm^2 molecule^{-1} s^{-1}$ , that is, approximately seven times slower than for the formation of the  $C_{2v}$  isomer. Since the energetics of each pathway are similar, the difference in formation rates must be reconciled by understanding the mechanisms of formation of the  $CO_3$  isomers. An oxygen atom reacting with a carbon dioxide molecule can

attack at a variety of reaction geometries. According to Mebel et al.<sup>[18]</sup>, an oxygen atom approaching carbon dioxide with  $C_{2v}$  symmetry is attractive on two of the five degenerate  $O(^1D)$  surfaces and forms a  $O...CO_2$  reaction complex that is calculated to be  $28 kJ mol^{-1}$  below the separated reactants. This complex can then proceed over a transition state, resulting in the formation of the  $C_{2v}$  carbon trioxide molecule where the energy barrier is either slightly below or slightly above the  $O(^1D) + CO_2(X^1\Sigma_g^+)$  reactants, depending on the calculation approach. However, in the previous work<sup>[18]</sup>, a direct pathway to

$CO_3(D_{3h})$  was not found. Our current calculations indicate that when an oxygen atom approaches  $CO_2$  with a  $C_{2v}$  symmetry (along the bisector of the  $OCO$  angle), there is a significant barrier, leading to  $CO_3(D_{3h})$  on all five electronic states correlating to  $^1D$ . However, since both isomers and the transition state separating them lie well below  $O(^1D) + CO_2(X^1\Sigma_g^+)$  in energy, it is possible that reaction trajectories exist that lead directly to  $D_{3h}$  bypassing the transition state. Such trajectories could start from the barrierless nonsymmetric approach ( $C_s$  symmetric) and then bifurcate in the vicinity of the transition state; some



of these will go to the cyclic structure and others to the  $D_{3h}$  isomer. The cone of acceptance for an oxygen atom adding across one of the two double bonds forming the  $C_{2v}$  isomer is probably larger than the cone of acceptance for the reaction to the  $D_{3h}$  isomer, which is consistent with the faster rate constant derived for the formation of the  $C_{2v}$  isomer. The rate constant for the destruction of  $CO_3(D_{3h})$  is  $1.8 \times 10^{-4} \text{ s}^{-1}$  ( $k_{-3}$ ). The  $D_{3h}$  isomer may also be produced by isomerization of the  $C_{2v}$  structure. Therefore, the forward and reverse isomerization channels between the  $C_{2v}$  and  $D_{3h}$  structures are included in the reaction model (Figure 4). The energy difference between the two isomers is  $0.4 \text{ kJ mol}^{-1}$  with the  $C_{2v}$  structure only slightly lower in energy. With the low energy barrier for interconversion between these structures ( $18.4 \text{ kJ mol}^{-1}$  relative to the  $C_{2v}$  structure) and the excess internal energy resulting from the formation of the  $CO_3$  isomers [Eqs. (3) and (4)], isomerization between the  $D_{3h}$  and  $C_{2v}$  structures should readily occur. The column densities of the two  $CO_3$  isomers are found to be insensitive to the rate constants  $k_4$  and  $k_{-4}$  with the current reaction model. This indicates that the formation of both  $CO_3$  isomers in our low-temperature samples is only dependent on  $CO_2+O$  reactions [Eqs. (3) and (4)] and that the destruction channels to  $CO_2+O$  ( $k_{-2}$  and  $k_{-3}$ ) are more important than the isomerization channels. This does not imply that isomerization does not take place, only that these channels are insignificant when compared to the formation and destruction channels indicated by Equations (3) and (4). To reproduce the column density of  $CO_3(C_{2v})$  near the latter part of the irradiation phase a higher-order formation pathway is required. A reaction between carbon monoxide and molecular oxygen can form carbon trioxide ( $C_{2v}$ ); this reaction is calculated to be exoergic by  $58.1 \text{ kJ mol}^{-1}$  (Figure 4).<sup>[24]</sup> The rate constant for this reaction ( $k_5$ ) is  $2.6 \times 10^{-20} \text{ cm}^2 \text{ molecule}^{-1} \text{ s}^{-1}$ . This is over three orders of magnitude slower than the formation of the  $C_{2v}$  isomer via  $CO_2+O$  ( $k_2$ ); also the reactants are much less abundant than those in Equation (3). This indicates that the reaction of carbon monoxide with molecular oxygen plays a minimal role in the formation of  $CO_3(C_{2v})$  but it is still required to reproduce the column densities observed in the experiment. A pathway to form molecular oxygen ( $O_2$ ,  $X^3\Sigma_g^-$ ) via recombination of two oxygen atoms ( $O$ ,  $^3P/1D$ ) is added to make the reaction model consistent. This reaction rate constant ( $k_6$ ) is  $2.8 \times 10^{-10} \text{ cm}^2 \text{ molecule}^{-1} \text{ s}^{-1}$ .

### 3. Conclusions

To summarize, our low-temperature spectroscopy experiments combined with the electronic structure calculations identify for the first time the hitherto elusive  $D_{3h}$  isomer of the carbon trioxide molecule together with its isotopomers. A self-consistent reaction model has been proposed to verify the formation and destruction of both the  $C_{2v}$  and the  $D_{3h}$  symmetric carbon trioxide isomers. The formation of the  $D_{3h}$  structure in the atmospheres of Earth, Mars, and Venus can occur via isomerization of the  $C_{2v}$  structure as previously proposed<sup>[7,18,19]</sup> or by a novel, previously unconsidered, one-step formation route via Equation (3). The inclusion of the newly discovered pathway in at-

mospheric reaction models may help to better explain the hitherto not fully resolved isotope enrichment of  $^{18}O$  in stratospheric carbon dioxide and provides an alternative channel for the  $O(^1D)$  quenching mechanisms. The  $CO_3(D_{3h})$  molecule is also probably produced in carbon dioxide ices that are exposed to space radiation such as those on interstellar dust grains, Triton or Mars, or in comets; our laboratory band assignments may help guide astronomical searches for the  $CO_3(D_{3h})$  molecule in these environments. Recognition of the  $D_{3h}$  isomer of carbon trioxide as a potential precursor to a more-complex atmospheric oxygen chemistry is important as it may also help constrain physical properties of the  $CO_3$  anion ( $CO_3^-$ ), which seems to have similar possible isomeric configurations to the neutral molecule.<sup>[25]</sup> The  $CO_3$  anion is one of the most important negative ions in the atmospheres of Earth and Mars and is a terminal ion in atmospheric chemistry.<sup>[26,27]</sup> Also, identification of the  $CO_2+O$  reaction pathways may help explain the isotope exchange in the isoelectronic reaction of oxygen atoms with dinitrogen monoxide ( $N_2O$ ) reaction, leading to the  $^{18}O$  enrichment of  $N_2O$  found in the Earth's stratosphere.<sup>[28,29]</sup>

### Acknowledgements

This material is based upon work supported by the National Aeronautics and Space Administration through the NASA Astrobiology Institute (Cooperative Agreement no. NNA04CC08 A issued through the Office of Space Science) and by the Air Force Office of Scientific Research (AFOSR; W911NF-05-1-0448). The authors would like to thank Ed Kawamura (University of Hawaii, Department of Chemistry) for electrical and mechanical work. We also thank Prof. Michael Frenklach (UC Berkeley) for providing the computer code utilized in solving the kinetics for our reaction models.

**Keywords:** atmospheric chemistry • kinetics • reactive intermediates • matrix isolation • molecular dynamics

- [1] J. Crovisier, *Earth, Moon and Planets* **1997**, 79, 125.
- [2] P. A. Gerakines, D. C. B. Whittet, P. Ehrenfreund, A. C. A. Boogert, A. G. G. M. Tielens, W. A. Schutte, J. E. Chiar, E. F. van Dishoeck, T. Prusti, F. P. Helmich, Th. De Graauw, *Astrophys. J.* **1999**, 522, 357.
- [3] *Photochemistry of Planetary Atmospheres* (Eds.: Y. L. Yung, W. B. DeMore), Oxford University Press, New York, **1999**.
- [4] Y. L. Yung, A. Y. T. Lee, F. W. Irion, W. B. DeMore, J. Wen, *J. Geophys. Res.* **1997**, 102, 10857.
- [5] D. Katakis, H. Taube, *J. Chem. Phys.* **1962**, 36, 416.
- [6] W. B. DeMore, C. Dede, *J. Phys. Chem.* **1970**, 74, 2621.
- [7] M. J. Perri, A. L. Van Wyngarden, J. J. Lin, Y. T. Lee, K. A. Boering, *J. Phys. Chem. A* **2004**, 108, 7995.
- [8] N. G. Moll, D. R. Clutter, W. E. Thompson, *J. Chem. Phys.* **1966**, 45, 4469.
- [9] M. E. Jacox, D. E. Milligan, *J. Chem. Phys.* **1971**, 54, 919.
- [10] C. J. Bennett, C. Jamieson, A. M. Mebel, R. I. Kaiser, *Phys. Chem. Chem. Phys.* **2004**, 6, 735.
- [11] Y. L. Yung, W. B. DeMore, J. P. Pinto, *Geophys. Res. Lett.* **1991**, 18, 13.
- [12] T. M. Gamo, M. Tsutsumi, H. Sakai, T. Nakazawa, M. Tanaka, H. Honda, H. Kubo, T. Itoh, *Tellus* **1989**, 41B, 127.
- [13] V. Barth, A. Zahn, *J. Geophys. Res.* **1997**, 102, 12995.
- [14] M. C. Liang, F. W. Irion, J. D. Weibel, C. E. Miller, G. A. Blake, Y. L. Yung, *J. Geophys. Res.* **2006**, 111, D02302.
- [15] M. B. McElroy, D. M. Hunten, *J. Geophys. Res.* **1970**, 75, 1188.
- [16] D. S. Sethi, A. L. Smith, *Planet. Space Sci.* **1975**, 23, 661.

- [17] W. B. DeMore, *J. Geophys. Res.* **1970**, *75*, 4898.
- [18] A. M. Mebel, M. Hayashi, V. V. Kislov, S. H. Lin, *J. Phys. Chem. A* **2004**, *108*, 7983.
- [19] D. L. Baulch, W. H. Breckenridge, *Trans. Faraday Soc.* **1966**, *62*, 2768.
- [20] DALTON, release 1.2 (2001), a molecular electronic structure program written by: T. Helgaker, H. J. Aa. Jensen, P. Jørgensen, J. Olsen, K. Ruud, H. Ågren, A. A. Auer, K. L. Bak, V. Bakken, O. Christiansen, S. Coriani, P. Dahle, E. K. Dalskov, T. Enevoldsen, B. Fernández, C. Hättig, K. Hald, A. Halkier, H. Heiberg, H. Hettema, D. Jonsson, S. Kirpekar, R. Kobayashi, H. Koch, K. V. Mikkelsen, P. Norman, M. J. Packer, T. B. Pedersen, T. A. Ruden, A. Sanchez, T. Saue, S. P. A. Sauer, B. Schimmelpfenning, K. O. Sylvester-Hvid, P. R. Taylor, O. Vahtras.
- [21] Recall that these rate constants are derived for reactions at 10 K. However, it is not the goal of this paper to determine absolute rate constants but rather to identify the elusive  $D_{3h}$  isomer and to develop a kinetically consistent reaction model to identify and understand the reaction pathways and their associated mechanisms that are relevant for the formation of the carbon trioxide isomers.
- [22] M. Frenklach, H. Wang, M. J. Rabinowitz, *Prog. Energy Combust. Sci.* **1992**, *18*, 47.
- [23] The branching ratio for either  $O(^3P)$  or  $O(^1D)$  reacting with carbon dioxide to form  $CO_3(C_{2v})$  is unknown. However, as noted from PES calculations, the  $O(^3P) + CO_2$  reaction has a barrier and must also undergo intersystem crossing (ISC) to achieve the ground state  $CO_3(C_{2v})$  product on the singlet surface.
- [24] B. M. Elliot, A. I. Boldyrev, *J. Phys. Chem. A* **2005**, *109*, 3722.
- [25] C. D. Cappa, M. J. Elrod, *Phys. Chem. Chem. Phys.* **2001**, *3*, 2986.
- [26] J. Wisemberg, G. Kockarts, *J. Geophys. Res.* **1980**, *85*, 4642.
- [27] G. J. Molina-Cuberos, H. Lichtenegger, K. Schwingenschuh, J. J. Lopez-Moreno, R. Rodrigo, *J. Geophys. Res.* **2002**, *107*, 5027.
- [28] M. B. McElroy, D. B. A. Jones, *Global Biogeochem. Cycles* **1996**, *10*, 651.
- [29] Y. L. Yung, M. C. Liang, G. A. Blake, R. P. Muller, C. E. Miller, *Geophys. Res. Lett.* **2004**, *31*, L19 106.

---

Received: June 27, 2006

Published online on October 9, 2006